An artificial seabed carpet for multidirectional and broadband wave energy extraction: Theory and Experiment

Marcus Lehmann*, Ryan Elandt*, Henry Pham*, Reza Ghorbani†, Mostafa Shakeri* and Mohammad-Reza Alam*
*Department of Mechanical Engineering, University of California, Berkeley
marcus.lehmann@berkeley.edu, relandt@berkeley.edu, reza.alam@berkeley.edu
†Department of Mechanical Engineering, University of Hawaii

***Abstract*— It has been reported worldwide that muddy seafloors can extract a significant fraction of the energy stored in overpassing ocean waves within several wavelengths. We consider a synthetic-seabed-carpet, supported by multiple springs and generators, that should extract wave energy the same way as muddy seafloor does. This paper presents the analytical model, the construction of the first working prototype and the experimental results of this novel concept called the Carpet of Wave Energy Conversion (CWEC). We successfully demonstrated its capability to absorb and convert wave energy for multiple sea states. As the CWEC operates completely submerged, it imposes no threat for overpassing ships and has no effect on oceanfront scenes. The CWEC's orientation combines the advantages of a point absorber, an attenuator and a terminator: it is wave-direction-independent, has a high absorption efficiency and can be exposed to high wave energy flux with its flexible spread perpendicular to the wave-propagation direction.**

The ability to cancel waves can be used to create safe zones in the ocean, prevent erosion and protect harbors. Secondly, the CWEC's primary energy conversion creates seawater at high pressure. This can be used to generate electricity, be used for desalination and for the distribution of fresh water. High pressure water can supply pumped-storage hydroelectric power plants, which are the most efficient way to balance the electrical grid.

***Index Terms*—Wave energy, Wave Energy Converter (WEC), Synthetic Seabed, Shallow Water Device, Carpet of Wave Energy Conversion (CWEC)**

I. Introduction

One of the major engineering challenges of the 20th and 21st centuries is to meet the constantly increasing global energy demand. Approximately 3 billion people live within 200 km away from the coast and migration is likely to cause this number to double by 2025, see Creel [1]. And yet, the resources provided by the ocean are hardly being used. Mork et al. [2] have calculated a worldwide theoretical wave power potential of 29,500 TWh/year where the power densities occur from 50 to 125 kW/m at latitudes greater and lower than 40 degrees from the equator. Locations within these areas are preferred to harvest this energy potential with Wave Energy Converts (WEC). Drew et al. [3] emphasize the advantage of the natural seasonal variability of wave energy, which follows the electricity demand distributed over the year.

Inspired by nature, Alam [4] introduced a novel WEC concept that uses a synthetic seabed carpet to imitate the absorption behavior of muddy seafloors. The inspiration comes from worldwide reports that muddy seafloors can extract a significant fraction of the energy stored in overpassing ocean waves [5]. For example, accretion of mud banks in the Gulf of Mexico (referred to by locals as mud hole) have created an area where even strong waves are damped within just a couple of wavelengths. Thus, a synthetic seabed carpet supported by springs and generators, see Figure 1, is expected to extract a comparable amount of energy by responding to the action of overpassing waves in the same way the mud does.

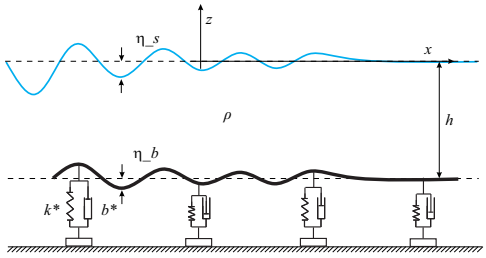

Fig. 1: Schematic of a synthetic viscoelastic carpet on the seafloor for extracting energy from surface gravity waves. The carpet is composed of linear springs with the stiffness coefficient k^* that provide the restoring force, and generators modeled by dash-pot type dampers with damping coefficient b^* that extract energy. The distance between each module of the spring damper is assumed much smaller than the typical wavelength of overpassing waves such that the assumption of continuously distributed spring dampers is valid.

The subject of this paper is the theoretical and experimental investigation of this synthetic seabed carpet, called the Carpet of Wave Energy Conversion (CWEC). This paper describes the constructional steps needed to transfer the carpet concept into a first working prototype and presents experimental results of the developed converter while operating under the influence of several sea states.

This system is governed by a nonlinear and coupled set of equations that include the dynamics of gravity waves and the visco-elastic seabed. The linearized form of the governing equations admit a surface-mode and a bottom-mode eigen

solution. While damping of surface-mode waves is higher for longer waves (and is therefore classic), the damping of a bottom-mode wave is higher for shorter waves. Furthermore, computational investigation of nonlinear interactions of surface waves and the carpet have shown that the rate of energy extraction increases for steeper surface waves, see Alam [6].

Section II provides the governing equations that describe the analytical model. Section III describes the engineering design, the steps taken from the abstract model to the first working prototype, and the constructional solution of the required components of the system. Section IV presents the experiments conducted and their results. The discussion in Section V emphasizes the advantages of the CWEC and provides an outlook of the system. Concluding, Section VI summarizes the presented research.

II. Analytical Modeling

Alam [6] describes the behavior of an actuated seafloor-mounted carpet for a high-performance wave energy extraction. We consider a homogeneous inviscid incompressible fluid with irrotational motion. The bottom at the mean depth z = -h, see Figure 1, is viscoelastic. The equations of the velocity potential ϕ and the surface and bottom elevations η_s and η_b ignore the surface tension and read:

$$\nabla^2\phi = 0, \quad -h+\eta_b < z < \eta_s \tag{1}$$

$$\eta_{s,t} + \eta_{s,x}\phi_x = \phi_z, \quad z = \eta_s, \tag{2}$$

$$\phi_t + \frac{1}{2}(\phi_x^2+\phi_z^2) + g\eta_s = 0, \quad z = \eta_s, \tag{3}$$

$$\eta_{b,t} + \eta_{b,x}\phi_x = \phi_z, \quad z = -h+\eta_b, \tag{4}$$

$$\phi_t + \frac{1}{2}(\phi_x^2+\phi_z^2) + g\eta_b + \frac{P_b}{\rho} = 0, \quad z = -h+\eta_b, \tag{5}$$

$$b^*\eta_{b,t} + k^*\eta_b + P_b = 0, \quad z = -h+\eta_b \tag{6}$$

with the gravity acceleration g, the density of the fluid ρ, the pressure on the seabed P_b, the viscous damping b^* and the stiffness coefficient of the viscoelastic bottom per unit area k^*. The linearized form of governing equations admits a propagating wave in the form of

$$\eta_s = a_s\, e^{i(kx-\omega t)}, \tag{7}$$

$$\eta_b = a_b\, e^{i(kx-\omega t)}, \tag{8}$$

$$\phi = (A\, e^{kz} \;+\; B\, e^{-kz})\, e^{i(kx-\omega t)} \tag{9}$$

where

$$a_b = a_s \cosh kh \left(1 - \frac{gh\,\tanh kh}{\omega^2}\right), \tag{10}$$

$$A = -ia_s\frac{\omega^2+gk}{2k\omega}, B = i\,a_s\frac{\omega^2-gk}{2k\omega}, \tag{11}$$

with the surface amplitude a_s and the bottom amplitude a_b. Furthermore, the dispersion relation reads in dimensionless form

$$\gamma\Omega^4\tanh(\mu) + i\mu\gamma\zeta\Omega^3 - \mu\Omega^2 - i\mu^2\gamma\zeta\Omega\tanh(\mu) + \mu^2(1-\gamma)\tanh(\mu) = 0 \tag{12}$$

The dimensionless variables are

$$\Omega = \omega\sqrt{h/g}, \quad \zeta = \frac{b^*}{\rho\sqrt{gh}}, \quad \gamma = \frac{\rho g}{k^*}, \text{ and } \mu = kh \tag{13}$$

with the dimensionless frequency Ω, the dimensionless damping ratio ζ, the dimensionless restoring force γ and the shallowness μ.

The average energy stored in one piston damper over one period of time is

$$\overline{E_p} = \int_0^T F_p \cdot v_p\, dt = \int_0^T b\,\omega^2 a_b^2\, cos^2(\omega t)\, dt = \frac{2\pi^2\, b\, a_b^2}{T} \tag{14}$$

with $v_p = \omega\, a_b\, cos(\omega t)$

where a_b is the amplitude of the bottom and b the damping coefficient of the pump.

The energy stored in the carpet per unit area for a undamped system is described as

$$E_{tot} = E_{kin} + E_{pot} = \frac{1}{2}\rho g a_s^2 D \tag{15}$$

with

$$E_{kin} = \frac{1}{2}\rho g a_s^2 \left\{\frac{\sinh 2kh}{2}\left(\frac{\omega^2}{gk}+\frac{gk}{\omega^2}\right) - 2\sinh^2 kh\right\} \tag{16}$$

$$E_{pot} = \frac{1}{4}\rho g(a_s^2 - a_b^2) + \frac{1}{4}k^* a_b^2 \tag{17}$$

and the dimensionless constant D

$$D = \frac{\sinh 2kh}{2}\left(\frac{\omega^2}{gk}+\frac{gk}{\omega^2}\right) - 2\sinh^2 kh + \frac{a_s^2-a_b^2}{a_s^2} + \frac{k^* a_b^2}{2\rho g a_s^2} \tag{18}$$

$$E_{tot} = \frac{1}{2}\rho g a_s^2 \left\{\frac{\sinh 2kh}{2}\left(\frac{\omega^2}{gk}+\frac{gk}{\omega^2}\right) - 2\sinh^2(kh) + \rho g(a_s^2-a_b^2) + k^* a_b^2\right\} \tag{19}$$

The solution of 12 gains an imaginary part $\omega = \omega_r + i\omega_i$ if damping is present. The dimensionless constant D is then written as D_d

$$D_d = \frac{1}{2}\left(\frac{\sinh(2\mu)}{2}\left(\frac{\Omega\_r^2}{\mu}+\frac{\mu}{\Omega\_r^2}\right) - 2\sinh(\mu)^2\right)$$

$$+\frac{1-\alpha}{2}+\frac{\alpha}{2\gamma} \tag{20}$$

where Ω_r is the real part of the dimensionless Ω and the dimensionless amplitude ratio of bottom to surface

$$\alpha=\frac{a_s^2}{a_b^2}=\cosh^2\mu\,(1-\frac{\mu\tanh\mu}{\Omega^2}) \tag{21}$$

with $a_s(t)=a_{s0}\,e^{\omega_i t}$. The energy in dimensionless form is then written as

$$\epsilon=\frac{E}{E_0}=\frac{1}{2}e^{2\Omega_i\,\tau}\,D_d \tag{22}$$

with $E_0=1/2\rho g a_s^2$ and $\tau=t\,\sqrt{\frac{g}{h}}$

The energy in the carpet for one period of time is then

$$E_c=\frac{1}{2}\,\rho\,g\,a_{s0}^2\,\epsilon\,A_c \tag{23}$$

where A_c represents the carpet area.

III. Experimental Modeling

This section describes the applied systems engineering methodology, based on [7] and its implementation to tackle the design challenge of developing a first working prototype based on the fundamentals provided by the analytical model described in chapter II. The approach divides the development process into five steps:

1) Problem description
2) Definition of specifications
3) Definition of components
4) Constructional solutions of components
5) Final assembly of the overall design

A. Problem description

To describe the problem in a solution-neutral manner, the problem is raised to the highest level of abstraction. Hence, the system is replaced by a black box placed on the ocean floor exposed to a sinusoidal pressure caused by the fluid above. The system boundaries are crossed by an energy flux into the system caused by the pressure field over the black box and by an energy flux out of the system, consisting of desired mechanically usable energy.

B. Definition of specifications

The second step is to describe the desired specifications and the defining figures of the design. The prototype is designed specifically for the testing facilities described in Section IV. The defining figures were as follows: a wave tank width of $0.45\,m$, a maximum water depth within the test area of $1\,m$, and a minimum possible wave length that is dependent on the final height of the design in the order of $2\,m$. This wavelength corresponds to a frequency of $0.88Hz$. To fulfill the conditions of the linear theory, shallowness ka and steepness a/h have to be less than 0.3. The wave number is defined as $k=2\pi/\lambda$.

The maximum amplitude of the surface a_s with the above given restrictions is $a_{s,max}=0.191\,m$. The amplitude of the bottom a_b is assumed to be in the order of the amplitude of a water particle at this depth and is thus calculated with the vertical displacement of water particles

$$\xi=a\frac{\sinh\,k(h+z)}{\sinh\,kh}. \tag{24}$$

At a water depth of $h=0.2\,m$ and a wave length of $\lambda=4\,m$, which are the desired height and length specifications of the experimental set up, the amplitude of the bottom is $a_b=0.0265m$. The dispersion relation provides the respective period T for this wavelength and the gravity constant $g=9.81\,m/s^2$.

$$T=2\pi(g\,k\,\tanh kh)^{-\frac{1}{2}}=1.67s \tag{25}$$

With the above given values, equation 14 and an expected damping coefficient in the order of $b^*=100\,Ns/m$, the average energy in the piston for one period equals $E_p=43.12\,J$.

The specifications of the overall system were the following:

- A modular design that allows multiple set ups in propagation direction of the wave
- Installation capability of the experimental set up in the wave tank
- Flexibility of stiffness and damping coefficients, carpet properties and Power Take Off (PTO) locations

The specifications of the absorber carpet were the following:

- Ability to maintain the pressure difference between fluid above and below the carpet while operating
- Ability to adopt to wave shape
- Maximum vertical displacement and bundling of the forces on the carpet of the connection points between carpet and PTO
- Water resistance and impermeability
- Secure connection between carpet and PTO

The specifications of the PTO system were the following:

- Ability to damp the vertical displacement of the absorber carpet
- Energy conversion capability
- Ability to operate submerged

C. Definition of components

In the third step, the black box was divided into four components, as shown in Figure 2. The required functionality of these components was defined to fulfill the requirements specified in the second step.

The novel design of this WEC consists of the four components “Absorber Carpet”, “Connection” , “Power Take Off System (PTO)” and “Mooring”. With their specifications determined, the four components operate together in sequence as follows: The “Absorber Carpet” bundles the absorbed energy of the impinging waves to the “Connection”, which transmits the energy to the hydraulic “PTO” units. “PTO” units convert the translational kinetic energy into a mechanically usable energy. The “Mooring” connects the bottom of the “PTO” units with the bottom of the tank.

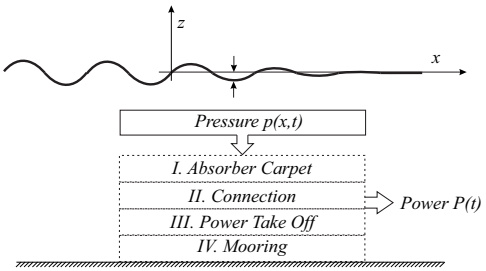

Fig. 2: Components

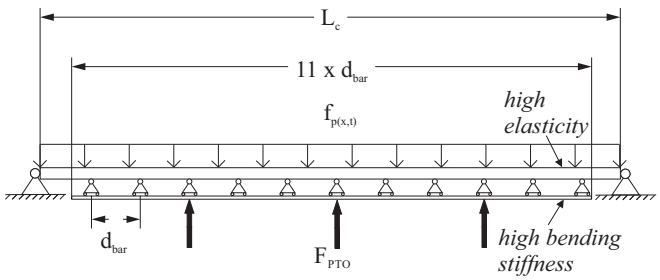

Fig. 3: Mechanical model of the Absorber Carpet

D. Constructional solutions of the components

In the fourth step constructional solutions for the four system components are developed.

1) Absorber Carpet: To fulfill the specifications of a continuous carpet, a material with anisotropic specification is needed. Along the x-axis an elastic material behavior, thus a low Young's modulus is desired to allow the carpet to change its initial length. As the PTO exerts a vertical force on the carpet, a sole elastic material would lead to a formation of nodes of the carpet with nodal points at the PTO units. As the converted energy is directly related to the displacement of the carpet at the position of the PTO units, no energy would be converted in this case. Thus, along the y axis a high bending stiffness is desired to avoid this nodal building.

One single material cannot fulfill these specifications. To solve this problem, the systems engineering method "Separation of Functionality" was used, which lead to the solution of a composite material, see [8]. The two specifications are met separately by individual materials connected with each other. Figure 3 shows the mechanical model of this composite material, where $f_{p(x,t)}$ represents the area force caused by the pressure field above and F_{PTO} represents the damping force caused by the PTO units, for this case at three equally distributed locations.

The low Young's modulus is provided by a continuous material with the desired properties and the length L_c. For the continuous material natural rubber with a thickness of 0.635 cm and a Young's modulus of 0.0045 GPa was selected.

A second material acting as a bending beam is connected via eleven roller supports located at the distance d_{bar} to each other with the first material. Fiberglass with a bending stiffness of 31 Nm^2 was selected for the beam material.

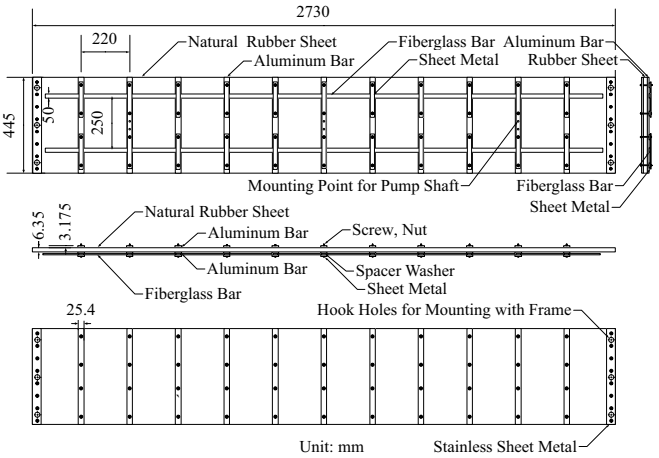

Fig. 4: Technical Drawing of the Absorber Carpet

Waves overpassing the carpet cause a time dependent pressure on the unit area of the carpet and thus exerting the area force $f_p(x,t)$. The fiberglass stiffens out the carpet and transmits the area force to the PTO points. Figure 4 shows the technical drawing of the implemented design of the composite carpet.

In our constructional implementation of the mechanical model, one roller support connecting the carpet to the PTO is built as follows: Two aluminum bars squeeze the natural rubber in between, secured by bolts and nuts. The aluminum bar underneath the carpet serves as the physical connection to the upper surface of the fiberglass, placed perpendicular to each other. The lower surface of the fiberglass is in physical contact with a sheet metal. The sheet metal is rigidly connected with the aluminum bar using bolts and nuts. Spacer washers placed between the aluminum bar and the metal sheets leave enough space for the fiberglass to move perpendicular to the aluminum-bar/sheet-metal clamp.

2) Connection: The shaft connecting the carpet to the PTO uses a direct physical connection with a aluminum bar below the carpet.

3) Power Take Off System (PTO): Among the available solutions for WEC PTO systems, we decided to implement an hydraulic PTO for the reasons given in Section V. The PTO uses two single acting reciprocating positive displacement pumps that operate in opposite directions using vertically acting piston shafts. Thus, one entire PTO unit operates in double acting manner, dampening the Absorber Carpet in both upward and the downward motions. The pumps chosen for the prototype have a volume per stroke of 67.0 ml at a stroke length of $l_{stroke} = 0.11\,m$. The damping coefficient of the pump in the velocity range of the carpet of $0.036\,m/s$ is in the order of $b_{pump} = 240\,Nsec/m$.

Based on experiments with the selected pumps, the degree of efficiency of one pump is calculated to about 10%. Evaluation of the overall PTO system have shown, that the efficiency of the pump is the primary limiting factor for the entire PTO system. To reduce pipe losses, the feeding diameter of the

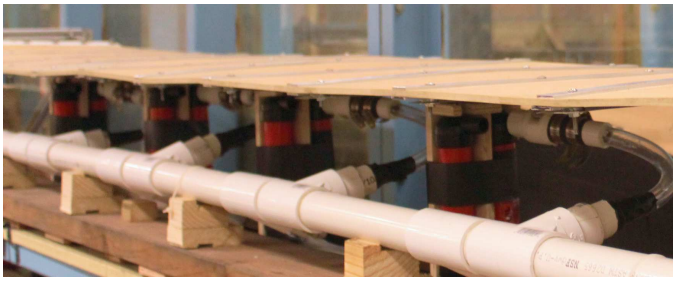

(a) The white PCV pipe connects all ten pumps (red cylinder) with the PTO discharge where the generated flux is measured. Two pumps are creating one double reacting PTO unit.

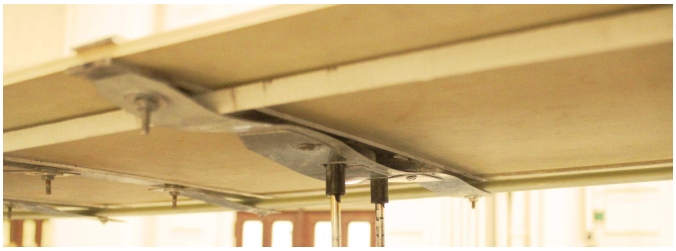

(b) The Absorber Carpet is made out of natural rubber (beige rubber). The rubber is clamped by aluminum bars from top and below in the distance d_{bar}. Every pair of bars serves as a connection point for the sliding support which connects the fiberglass and the rubber. Additionally it serves as a connection point for the pump shafts at the respective segment positions.

Fig. 5: Final assembled carpet components.

pump outlet is never undershot in the entire hydraulic system. The diameter of the PTO pipe was selected to be 3.175 cm.

4) Mooring: The Mooring connects the PTO units to the bottom of the tank with a hinge that allows the PTO units to rotate around the y-axis. As the carpet adopts the motion of the overpassing waves, the top of the piston shafts will be displaced in z- and in x-direction, see 1. Thus the PTO units require the ability to rotate around the y-axis.

E. Final assembly of the overall design

In the fifth step, the four components are brought together in the final assembly of the overall design. Figure 5 shows the assembled constructional solution in the frame of the experimental set up outside the tank. The white PVC pipe connects all ten pumps (red piston) with the PTO discharge where the generated flux is measured. The Absorber Carpet (beige rubber) is segmented through the supporting aluminum bars clamping onto the carpet from above and below.

IV. Description of conducted experiments

To cross-validate the theoretical and computational results as well as to study the performance of the CWEC under the action of highly nonlinear surface waves, we conducted a detailed set of 2D experiments, see [9]. Experiments were performed in the wave tank (L x W x D=30 x 0.45 x 2.4 meter) at the University of California, Berkeleys OBrian hall, using a flap-type wave-maker to simulate several sea-states. The set up as described in Section III was used for the experiments.

The performance criteria used to evaluate the functionality of the operating system are the total efficiency of the PTO η_{PTO} and the absorption efficiency of the carpet η_{abs}. Figure 6 gives an overview of the experimental set up and its parameters. The Absorber Carpet and its hydraulic PTO units are held in place by a frame connected to the bottom of the tank. Restriction of the experimental facilities could not entirely prevent fluid motion under the carpet caused by the impinging waves. The total efficiency was calculated as the ratio of energy harvested from the PTO to the energy stored in the impinging waves. The amount of energy harvested was measured by the potential and kinetic energy of the flux measured at the PTO discharge at the height h_p.

Experiments were conducted to collect the required data to calculate the total efficiency and the absorption coefficient of the final set up while operating mounted on the bottom of the tank.

At the given water level of $h = 0.7\,m$ and a pump height of $h_p = 0.675\,m$, the flux of the PTO and the wave amplitude a_{in} and a_{out} were measured manually for several sea states. A beaker was placed at the height of h_p above the mean water level and the time needed for a volume of $3000\,ml$ pumped was stopped manually. The flux of the PTO is calculated as

$$V = \frac{V_{meas}}{t_{meas}} \tag{26}$$

The total efficiency of the PTO is calculated

$$\eta_{total} = \frac{P_{PTO}}{P_{wave}} \tag{27}$$

with

$$P_{PTO} = P_{pot} + P_{kin} = \rho V g h_p + \frac{1}{2}\rho V v_{free}^2 \tag{28}$$

where

$$v_{free} = \frac{V}{A_{out}} \tag{29}$$

The area of the free jet at the PTO discharge is $A_{out} = 1.2610^{-4}\,m^2$. The kinetic power of the free jet for the given experimental parameters is in the order of $10^{-10}\,W$ and is therefore negligible. The wave power converted by the CWEC is the power of the wave entering the control volume, which is set at the front of the experimental set up. The wave power is calculated as

$$P_{wave} = \frac{1}{2}\rho g C g a_{in}^2 W \tag{30}$$

with a wave tank width of $W = 0.45\,m$, wave amplitude of a_{in} before the wave reaches the set up, the gravity acceleration g, the density of water at room temperature of $\rho = 999\,kg/m^3$ and the group velocity of the wave

$$Cg = \frac{1}{2}\left(1 + \frac{2k}{\sinh 2kh}\right)\lambda f \tag{31}$$

With equation 28 and 30, the average total efficiency is calculated as

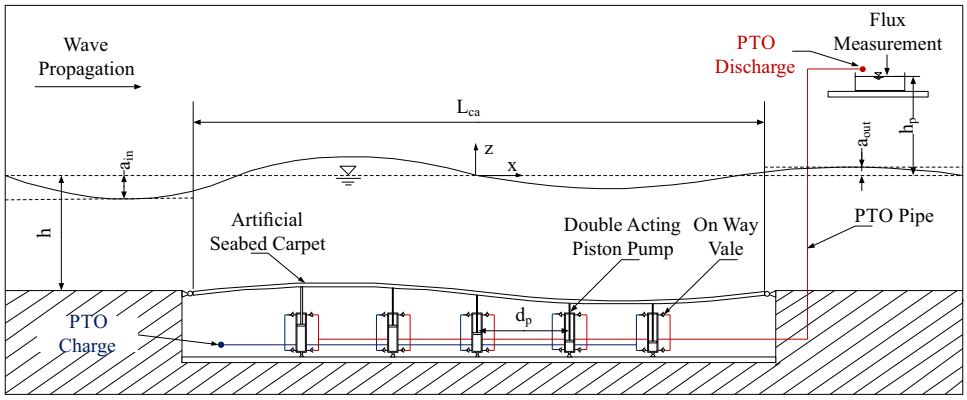

Fig. 6: Schematic of the experimental set up. The artificial seabed carpet is displaced by the overpassing waves impinging from the left side. The shafts of the double acting reciprocating positive displacement pumps are connected with the carpet and are displaced equally. Through the displacement of the piston, water is pumped from PTO charge to the PTO discharge. The flux at the discharge at the height h_p together with the wave amplitudes a_{in} and a_{out} are measured.

$$\eta_{total} = \frac{4Vh_p \sinh 2kh}{\lambda f W(a_{in}^2 - a_{out}^2)(\sinh 2kh + 2kh)} \tag{32}$$

The average total coefficient reflects the ability of the device to convert the energy of impinging waves into mechanically usable energy and thus specifies the quality grad of the primary energy conversion.

The absorption coefficient η_{abs} of the system is defined as

$$\eta_{abs} = \frac{E_{in}^2 - E_{out}^2}{E_{in}^2} = \frac{a_{in}^2 - a_{out}^2}{a_{in}^2} \tag{33}$$

The absorption coefficient reflects the ability of the device to diminish the energy of impinging waves.

The configuration for the following experimental results was a setup with three PTO units connected at the outer left and right and inner position, together with a bending stiffness of 4802.9 N/m. Figure 7(a) and Figure 7(b) are showing η_{PTO} and η_{abs} values for different wave steepnesses at a constant amplitude of impinging wave of $a_{in} = 0.09\,m$.

We were able to measured a peak PTO efficiency of 4.51 %. For lower kh values, a frequency dependent nodal building has been perceived. The lower efficiency values for these frequencies can be drawn back to the velocity dependent damping force caused by the pistons.

Figure 8(a) and Figure 8(b) are showing η_{PTO} and η_{ABS} values for different wave steepness's at a constant water depth of $h = 0.07\,m$.

Figure 9(a) and Figure 9(b) are showing η_{PTO} and η_{ABS} values for different wave steepness's at a constant wave number of $k = 2.03\,1/m$.

Figure 10 shows the experimental setup of the CWEC while operating under the influence of non linear waves. The figure illustrates the displacement of the carpet in z direction and the adoption of the wave shape.

The peak value of PTO efficiency measured is 5.64 % at a wave length of 2.03 meters, where the absorption efficiency was 82.4 %. The peak absorption efficiency in this data set

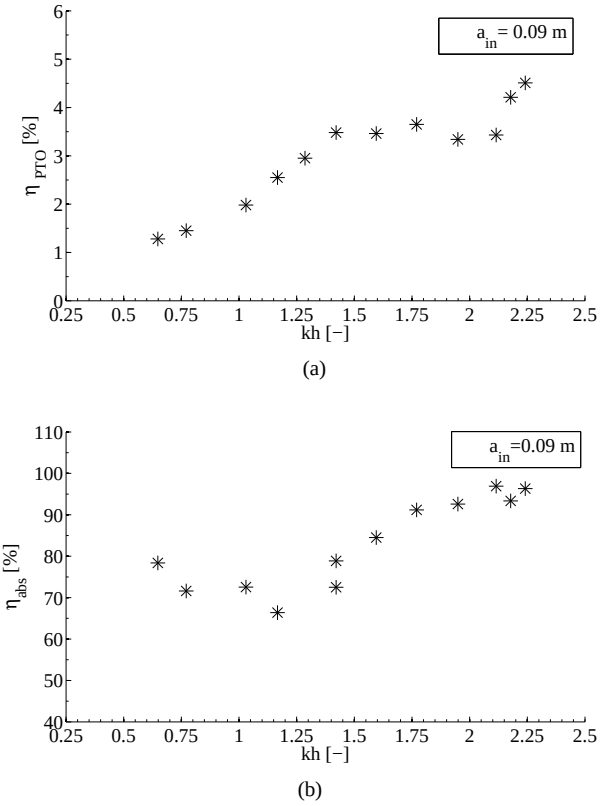

Fig. 7: Measured PTO efficiency (a) and absorption efficiency (b) for several shallowness values for a fixed wave amplitude of $a_{in} = 0.09\,m$

is 96.33 % for a wave length of 1.96 m which corresponds to a wave length carpet ratio of 1.39. Thus, we can conclude that absorption efficiency and PTO efficiency are not directly related to each other.

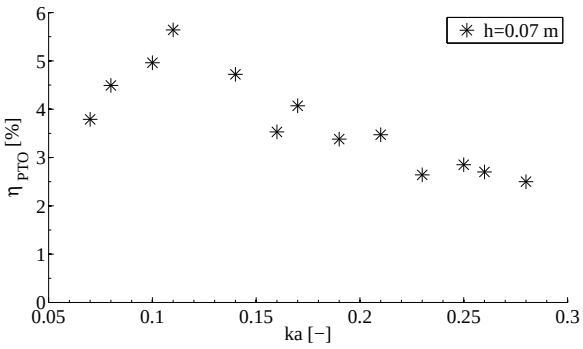

(a)

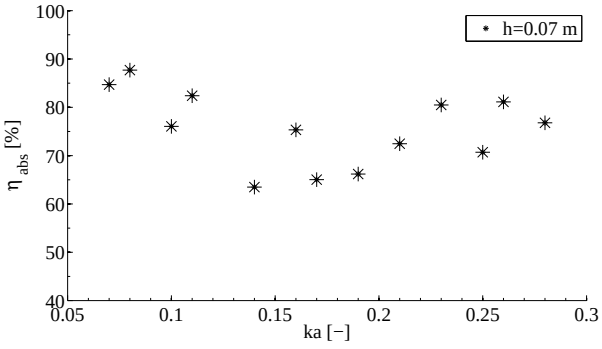

(b)

Fig. 8: Measured PTO efficiency (a) and absorption efficiency (b) for different wave steepness's at a constant water depth of $h = 0.07\,m$

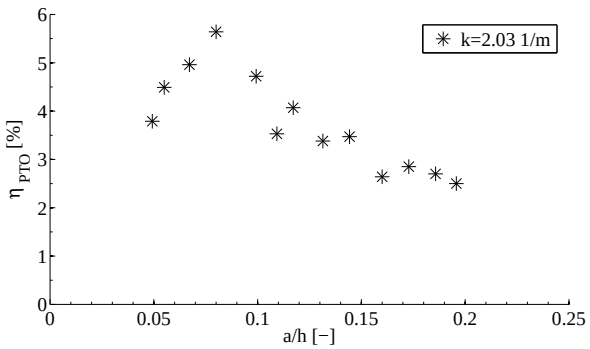

(a)

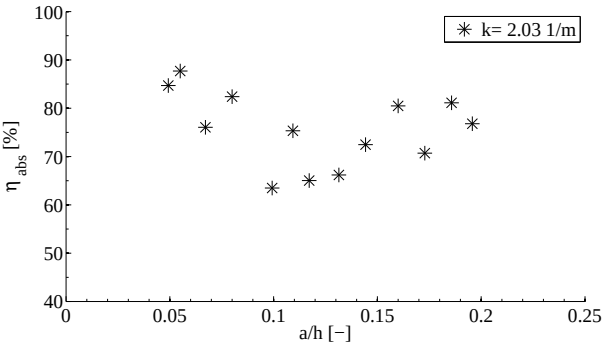

(b)

Fig. 9: Measured PTO efficiency (a) and absorption efficiency (b) for different wave steepness's at a constant wave number of $k = 2.03\,m$

V. Discussion

This novel design can be classified as a Wave Energy Converter with a nearshore, shallow water, bottom standing location; operating in heave, pitch motion, the converter's orientation is a combination of orientation attenuator and terminator.

Furthermore it combines the individual advantages of the three orientations types. The concept operates independent of wave direction like a point absorber, has a high absorption efficiency like a attenuator and can be extended arbitrarily perpendicular to the wave propagation direction, thus is exposed to a higher wave energy flux like a terminator.

The advantage of the overall design is the parallel usage of components, which significantly reduces the risk of failure of the entire system. Furthermore, a large scale system can be assembled only using many low cost industrial available components, which would reduce the maintenance costs while operating. A large scale CWEC placed in the ocean can be used to generate power and to cancel out waves.

The generated power in the form of high pressure water can be used: 1) to run a hydraulic turbine to generate electricity; 2) to supply a reverse osmosis process, which generates fresh water; 3) and to distribute fresh water. Nationwide, about 4 percent of U.S. power generation is used for water supply

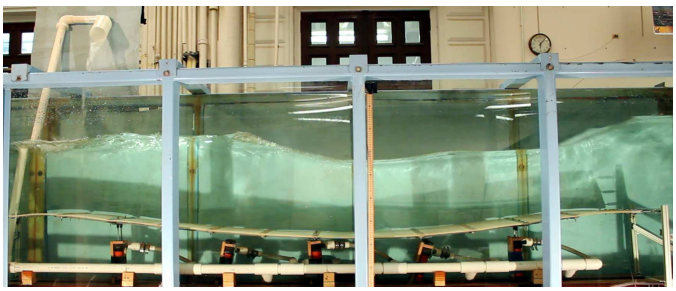

(a) Wave crests located above the outer PTO unit.

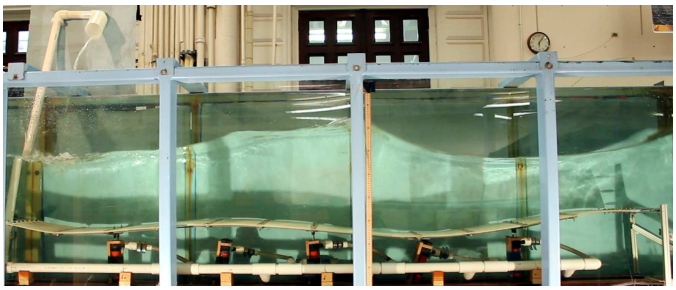

(b) Wave crests located above the central PTO units.

Fig. 10: Experimental set up while operating with 3 PTO units.

and treatment which corresponds to a per capita energy use for water supply and waste water treatment in 2000 of 123 Million MWh/a, see [10].

Furthermore, an increase of power supply by renewable energies will lead to imbalance in the electrical grid, as these power sources don't directly follow the demand for electrical power. Thus, energy storage technologies are becoming an important complementary necessity for the expansion of renewable energies. At the moment pumped-storage hydroelectric power plants have a maximum conversion efficiency of 65 to 80%, see [11], and are the most efficient way to store electrical energy at this scale. Compared to this, high pressure water stored in elevated reservoirs is converted to electricity by water turbines with a efficiency greater then 90%, see [12]. Around 5.8 to 10.2 % of the total U.S. electricity generation between 1990 and 2003 are supplied by hydro-power, see [10]. Thus, high pressure water stored in elevated reservoirs is an ideal way to store energy to buffer variations in the electrical grid.

A sample calculation for a large scale CWEC designed for application and operation in the ocean in the state of California with an average annual wave power flux of $30\,kW/m$, would produce in an optimum case the annual energy of $59.2GWh/a$. This case considers a carpet width perpendicular to the wave propagation of $50\,m$, an up time ratio of 0.9 and a PTO efficiency of 0.5. These values correspond an annual energy potential per meter carpet of $1.3\,GWh/am$ for the optimum case and $0.79\,GWh/am$ for a medium case with a PTO efficiency of 30%.

The next steps towards a commercial application of this novel concept in the ocean are 3-D wave tank test with larger scale optimized prototypes. The PTO efficiency of the tested system was limited by the efficiency of the used pumps with 10%. Thus, an optimized PTO unit using one double acting pump instead of two single acting pumps will reduce friction significantly and lead to higher PTO efficiencies.

The investigation of mechanical models like Maxwell or Zener compared to the Voigt model, which was used here, are of interested for next prototypes. These models are using more complex combinations of dampers and springs in series and parallel. Advantages of a hydraulic PTO system operating in an open cycle using ocean water or in a closed cycle using a hydraulic fluid are of interest, too.

VI. Conclusion

The main aim of the conducted research was the analytical modeling, the development of a first working prototype and experimental testing of the performance of the Carpet of Wave Energy Conversion (CWEC). This paper provides an analytical solution for the motion of a synthetic-seabed-carpet supported by multiple springs and generators, and the system's ability to extract energy. The process of transferring this novel wave energy converter concept to a first working prototype is set forth. The principle components of the prototype consist of a synthetic seabed carpet, a direct physical connection, a hydraulic Power Take Off system and a mooring system. The energy stored in overtopping waves is damped out by the absorber carpet and converted into hydraulic energy using double reacting reciprocating pumps which are connected to the carpet. The engineering challenge of an absorber carpet material with anisotropic material properties was addressed by using a composite material. The carpet material required the following properties: low Young's modulus in its horizontal direction and a high bending stiffness in its vertical direction. Natural rubber and fiberglass were selected to fulfill those requirements. The results of the experiments conducted are first data sets for the absorption and Power Take Off (PTO) efficiency while operating under the influence of several sea states. The functionality of the prototype was successfully tested and a PTO efficiency of 5.64 % and a peak absorption efficiency of 96.33 % could be achieved.

Acknowledgment

The first author also would like to thank the Theoretical and Applied Fluid Dynamics Laboratory at the University of California, Berkeley for the hospitality during his visit in 2012-2013, and Ritwik Gosh and the Machine Shop staff in the Department of Mechanical Engineering, UC Berkeley for their kind help.

We would like to thank Professor Evan Variano for helpful discussions during the conduct of the experiment. The financial support from the American Bureau of Shipping is gratefully acknowledged.

References

[1] L. Creel, "Ripple effects: Population and coastal regions," *POPULATION REFERENCE BUREAU*, vol. 12, no. 4, p. 500, 2003.

[2] M. P. G. Mork, S. Barstow and A. A. Kabuth, "Assessing the global wave energy potential," in *29 th International conference on Ocean, Offshore Mechanics and Arctic Engineering*, Shanghai, China, 2010.

[3] B. Drew, "A review of wave-energy converter technology," *Journal of Power and Energy*, vol. 223, 2009.

[4] M.-R. Alam, "A flexible seafloor carpet for high-performance wave energy extraction," in *Proceedings of OMAE 2012 31st International Conference on Ocean, Offshore and Arctic Engineering*, Rio de Janeiro, Brazil, 2012.

[5] G. S. A. Sheremet, "Observations of nearshore wave dissipation over muddy sea beds," *J. Geophys*, no. Res. 108, p. 111, 2003.

[6] M.-R. Alam, "Nonlinear analysis of an actuated seaoor-mounted carpet for a high-performance wave energy extraction," *Proceedings of the Royal Society*, 2012.

[7] G. Pahl, *Engineering Design: A Systematic Approach*. Berlin Heidelberg: Springer-Verlag, 2007.

[8] U. L. J. Ponn, *Konzeptentwicklung und Gestaltung technischer Produkte*. Berlin Heidelberg: Springer-Verlag, 2007.

[9] G. Payne, "Guidance for the experimental tank testing of wave energy converters," http://www.supergen-marine.org.uk/drupal/files/reports/WECtanktesting.pdf, 2008.

[10] U. D. of Energy, "Energy demands on water resources," http://www.sandia.gov/energy-water/docs/121-RptToCongress-EWwEIAcomments-FINAL.pdf, 2006.

[11] J. P. H. Ibrahima, A. Ilincaa, "Energy storage systemscharacteristics and comparisons," *Renewable and Sustainable Energy Reviews*, vol. 12, 2008.

[12] V. GmbH, "Hydro power," http://www.voith.com/en/markets-industries/industries/hydro-power-224.html, 2013.